Tree Physiology, 2024, **44**, tpae140
https://doi.org/10.1093/treephys/tpae140
Advance access publication date 7 November 2024
Research paper

Capturing drought stress signals: the potential of dendrometers for monitoring tree water status

Yanick Ziegler*, Rüdiger Grote, Franklin Alongi, Timo Knüver and Nadine K. Ruehr

Karlsruhe Institute of Technology, Institute of Meteorology and Climate Research - Atmospheric Environmental Research (KIT/IMK-IFU), Kreuzeckbahnstraße 19, 82467 Garmisch-Partenkirchen, Germany

*Corresponding author (yanick.ziegler@kit.edu)

Handling Editor: Dan Johnson

The severity of droughts is expected to increase with climate change, leading to more frequent tree mortality and a decline in forest ecosystem services. Consequently, there is an urgent need for monitoring networks to provide early warnings of drought impacts on forests. Dendrometers capturing stem diameter variations may offer a simple and relatively low-cost opportunity. However, the links between stem shrinkage, a direct expression of tree water deficit (TWD), and hydraulic stress are not well understood thus far. In this study, we exposed two widespread conifers *Pinus sylvestris L.* and *Larix decidua Mill.* to lethal dehydration by withholding water and closely monitored TWD, midday water potential (ψ) and midday stomatal conductance (g_s) under controlled greenhouse conditions. We found strong relationships between the three variables throughout the dehydration process, particularly suggesting the potential for continuous ψ predictions and stomatal closure assessments. However, the relationships decoupled during recovery from severe drought. We also identified TWD thresholds that signal the onset of drought stress and tissue damage, providing insights into stress impacts and recovery potential. While these findings are promising, challenges remain in practically transferring them to field set-ups by suitable TWD normalization. Importantly, we observed that midday g_s was drastically reduced when TWD persisted overnight, providing a directly applicable drought stress signal that does not require normalization. In conclusion, while challenges remain, our results highlight the potential of dendrometers for monitoring tree water dynamics. Implementing dendrometer networks could support the development of early warning metrics for drought impacts, enabling large-scale monitoring in diverse settings, such as urban areas and forest ecosystems.

Keywords: drought-recovery cycles, tree water deficit, water potential, *Pinus sylvestris*, *Larix decidua*.

Introduction

The frequency and severity of droughts are expected to increase with climate change (Spinoni et al. 2018, Suarez-Gutierrez et al. 2023), resulting in global tree damage and mortality (Allen et al. 2010, Senf et al. 2020, Yi et al. 2022), negatively affecting the carbon balance and ecosystem functioning (Choat et al. 2018). Water limitation immediately affects tree carbon sequestration through species-specific water control mechanisms. Regulation of stomatal conductance (g_s) reduces water loss at the expense of net photosynthesis (A_{net}). Severe droughts affect the hydraulic system of trees, resulting in poorly understood long-term legacy effects (Müller and Bahn 2022) and having lasting impacts on plant functionality and forest structures (Pretzsch et al. 2022).

Understanding the progressive impacts during and after drought enables adaptive measures. Monitoring tree physiological responses offers valuable information on species sensitivity and dependence on site properties, supporting management strategies such as selecting less susceptible species and timely irrigation in urban settings. However, appropriate techniques for operational tree water status monitoring are still not widely applied (Novick et al. 2022).

Usually, water potential (ψ) is measured to assess levels of drought stress. Generally, ψ gradients, primarily driven by soil water availability, leaf-level transpiration and cohesion forces (cohesion-tension theory; Dixon 1915), govern the water transport in vascular plants. Parameters such as ψ at which 50% of hydraulic conductivity is lost (P_{50}) provide insights into tree species' susceptibility to hydraulic damage (Choat et al. 2012). However, notable limitations exist: traditional pressure chamber measurements for ψ are complex (Rodriguez-Dominguez et al. 2022) and destructive sampling from tree canopies is necessary. Though valuable for stress indication, they are not continuous, and simultaneously monitoring multiple individuals requires substantial logistic effort. Thermocouple psychrometers provide continuous measurements but are complex, temperature-sensitive and not universally applicable, especially for resin-rich gymnosperms (Martinez et al. 2011, Novick et al. 2022).

Therefore, identifying mechanisms for continuous tree drought stress evaluation can vastly improve forest monitoring. A promising candidate is tree water deficit (TWD; Zweifel 2015, Steppe 2018, Salomón et al. 2022), derived from stem diameter variations monitored by dendrometers capturing μm-scales, which are already widely applied (e.g. TreeNet; Zweifel et al. 2021*a*), cost-efficient and non-destructive. TWD represents the decrease between actual and recorded maximum stem diameter (Zweifel et al. 2016, Knüsel et al. 2021). It is sensitive to environmental conditions like vapor pressure deficit (VPD) and soil water content (SWC) (Zweifel et al. 2005, Sánchez-Costa et al. 2015, Dunkleberger et al. 2023,

Received: June 12, 2024. **Accepted:** October 29, 2024

Oberhuber et al. 2023), water storage capacity of cell tissues (De Swaef et al. 2015) and water-use traits such as stomatal regulation (Drew et al. 2011, Liu et al. 2023). During the day, trees typically transpire more water than they can take up due to limitations in whole plant conductance or soil water availability, resulting in the mobilization of internal water reservoirs. On top of apoplastic water release (Mantova et al. 2022), symplastic water release from living elastic tissues (Knipfer et al. 2019), such as bark and phloem, results in turgor loss, reduction of cell volume and subsequent stem shrinkage (Zweifel et al. 2001, De Swaef et al. 2015, Steppe et al. 2015). While xylem shrinkage is often neglected, it can also contribute to reversible water release, largely depending on living cells within the xylem matrix (Skelton 2020, Oberhuber et al. 2023). With ample soil water, internal storage pools replenish at night, allowing stem diameter recovery or even a new maximum (Zweifel et al. 2021*b*). However, during periods of extended water limitation, growth is assumed to stop due to cell turgor losses inhibiting cell division and expansion (Zweifel et al. 2016, Krejza et al. 2022), while TWD accumulates, making it an indirect indicator of drought stress.

TWD is closely related to ψ (Cochard et al. 2001, Steppe et al. 2006, Drew et al. 2011, Peters et al. 2021, Lauriks et al. 2022), potentially enabling continuous ψ predictions (Dietrich et al. 2018) and stress monitoring. Additionally, TWD correlates with gas exchange, and TWD thresholds for plant mortality can be determined (Lamacque et al. 2020, Andriantelomanana et al. 2024). Knowledge of tree sensitivity thresholds can leverage existing data series, offering insights into the severity of past and current droughts.

However, the relations between TWD and physiological parameters have been evaluated within a limited range of species and drought-stress conditions, constraining their practical applicability. Most studies investigate mild drought conditions, excluding the impact of irreversible drought damage (Cochard et al. 2001, Drew et al. 2011, Dietrich et al. 2018). Under severe drought, dynamics might change as embolism events irreversibly release additional water from inelastic xylem conduits (Knipfer et al. 2019, Skelton 2020) and trigger the collapse of elastic cells (Mantova et al. 2022, Andriantelomanana et al. 2024). Understanding the ψ–TWD relationship during this critical phase is essential to indicate long-term damage (Vergeynst et al. 2015). Furthermore, correlations of TWD with gas fluxes are of interest but have received even less investigation than those with ψ. While ψ indicates the degree of drought stress and the current risk of irreversible damage, g_s represents plant functioning and possible carbon assimilation. Lastly, the impacts of stress release on the relationship between TWD and physiological parameters are currently unknown. Depending on drought severity, recovery pace varies among different physiological processes, with gas exchange parameters requiring more time compared with ψ (Ruehr et al. 2019, Rehschuh et al. 2020). If TWD recovery timing (Lamacque et al. 2020) does not match that of ψ and g_s, relationships decouple. Moreover, understanding how post-stress recovery dynamics affect susceptibility to future droughts is crucial to assessing forest functioning in a changing climate (Ruehr et al. 2019, Kannenberg et al. 2020).

Here we conducted a greenhouse study and exposed seedlings of two coniferous species, *Pinus sylvestris* and *Larix decidua*, to complete dehydration and variable rewetting. We chose the species due to their ecological relevance (Obojes et al. 2024) and their different strategies regarding water use, namely anisohydric vs isohydric behavior (Oberhuber et al. 2015). The experiment allowed us to analyze the relationships of TWD to midday ψ and g_s during drought progression and how stress release modifies these relationships. Specifically, we targeted the following questions: (i) how are TWD and ψ related during lethal drought progression; (ii) does the relationship between TWD and ψ change during recovery (after re-watering); (iii) how is TWD related to gas exchange during drought and recovery; and (iv) can we derive early-warning metrics on tree drought stress intensities based on TWD?

Materials and methods

Experimental setup

We conducted an experimental study in an environmentally controlled greenhouse facility at the KIT-Campus Alpin in Garmisch-Partenkirchen (708 *m* a.s.l., 47°28′32.9′ N, 11°3′44.2′ E) in June to August 2023. Three-year-old Scots pine (*P. sylvestris L.*) and European larch (*L. decidua Mill.*) seedlings ($n = 24$ per species) were obtained from a local tree nursery in Gunzenhausen, Germany, in March 2023 and planted in individual 5.7 L pots containing an organic clay substrate and perlite at a ratio of 5:1 supplemented with 6 g of slow-release fertilizer (Osmocote 5 8-9M, Micromax Premium; ICL Specialty Fertilizers, Geldermalsen, The Netherlands). On average, *P. sylvestris* seedlings were 79.3 ± 3.2 cm high and had a stem diameter of 15.5 ± 0.7 mm. For *L. decidua*, corresponding values were 79.0 ± 2.9 cm and 12.2 ± 0.7 mm, respectively.

We placed the seedlings inside the greenhouse compartment to acclimate to the new conditions 3 weeks before the experiment started and watered them to field capacity (twice a day 100 mL + individual watering if necessary). At the experiment start, the trees were assigned randomly to a control ($n = 6$ per species) or drought treatment ($n = 18$ per species) as depicted in Figure 1. The drought treatment included more trees to allow frequent sampling. The control trees further received water, while irrigation in the drought treatment was stopped during two drought phases and resumed during recovery. All drought-treated trees were first exposed to a 9-day drought period (D1). After a 3-day recovery phase, a second and more extended drought cycle followed (D2) until ψ ranged around the determined P_{50} values (see Table 1a), which took 28 days for *L. decidua* and 30 days for *P. sylvestris*. Then the drought treatment trees were equally and randomly distributed either to a drought–lethal or a drought–recovery treatment. To observe the full range of dehydration, the drought–lethal trees were further dehydrated until tree death occurred. In contrast, seedlings in the drought–recovery treatment were re-watered to investigate how the recovery potential after hydraulic damage occurrence develops.

Temperature and humidity (CS215, Campbell Scientific Inc., Logan, UT, USA), as well as photosynthetic active radiation (PAR; PQS 1, Kipp & Zonen, Delft, The Netherlands), were continuously measured half-hourly to verify stable conditions. Daytime air temperature was 23 ± 2 °C (mean ± SD), daytime VPD 1.0 ± 0.3 kPa (Figure S1 available as Supplementary data at *Tree Physiology* Online) and ambient light conditions in the greenhouse were supplemented by LED grow lamps (LED-KE 400 VSP, DHLicht, Wuelfrath, Germany) to ensure a constant PAR of $600 \pm 100 \frac{\mu mol}{s \cdot m^2}$ for 15

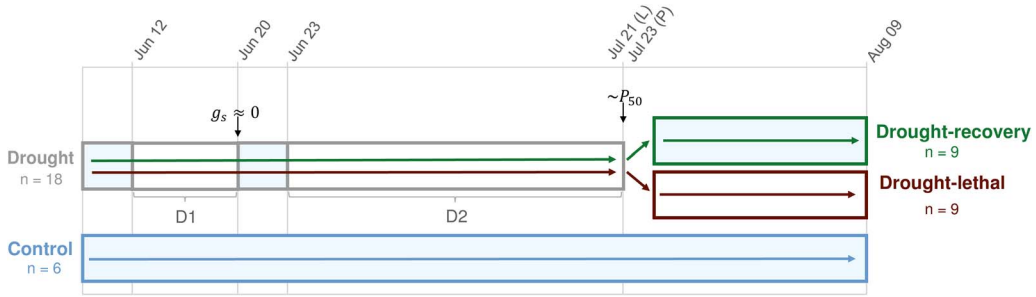

Figure 1. Overview of the experimental design. Shown are the drought and recovery cycles for *L. decidua* (L) and *P. sylvestris* (P) seedlings that were randomly assigned to a control ($n = 6$ per species) or drought treatment ($n = 18$ per species). We irrigated the trees to field capacity or withheld irrigation as depicted. In the first drought D1, we induced mild stress and re-watered all drought-trees once stomatal conductance approached $g_s \approx 0$. In the more extended drought D2, we aimed at inducing severe stress. Once water potentials (ψ) reached values representing hydraulic conductance losses of about 50% (P_{50}), we separated the drought treatment into a drought–recovery ($n = 9$ per species) that was re-watered and a drought–lethal treatment ($n = 9$ per species), which further dehydrated until tree death.

Table 1. Water potentials of vulnerability curve and stomatal closure thresholds for seedlings of *L. decidua* and *P. sylvestris*. (a) ψ at 12, 50 and 88% (P_{12}, P_{50}, P_{88}) percentage loss of conductance (PLC) and the according 95% confidence interval in brackets according to Figure S2 available as Supplementary data at *Tree Physiology* Online. (b) ψ at g_s of 5 and 50% relative to control means (ψ_{g5}, ψ_{g50}) and the according 95% confidence interval in brackets according to Figure S6 available as Supplementary data at *Tree Physiology* Online.

	Species	*L. decidua*	*P. sylvestris*
(a)	P_{12} [MPa]	−2.74 (−2.34/−3.06)	−2.52 (−2.32/−2.66)
	P_{50} [MPa]	−3.16 (−3.00/−3.24)	−3.11 (−3.04/−3.17)
	P_{88} [MPa]	−3.47 (−3.35/−3.63)	−3.58 (−3.45/−3.70)
(b)	ψ_{g5} [MPa]	−1.87 (−1.58/−2.23)	−1.33 (−0.91/−1.57)
	ψ_{g50} [MPa]	−1.06 (−0.62/−1.24)	−0.82 (−0.72/−0.88)

h a day. Trees were supplied with water using an automated irrigation drip system, and soil water content (SWC; UMS Water Content Sensor 10HS, 10-minute frequency; logger CR1000, Campbell Scientific, Inc.) was recorded for 10 trees per species (control $n = 2$, drought–recovery $n = 4$, drought–lethal $n = 4$).

Non-continuous measurements

Water potential

Midday water potential (ψ) was measured frequently between once a day and once a week, depending on the experimental phase with a pressure chamber (Model 600D, PMS Instruments, OR, USA; Scholander et al. (1965)). In the case of *L. decidua*, we sampled small twigs, and for *P. sylvestris*, we utilized needle fascicles to save plant material and maximize the number of possible measurements. For *P. sylvestris*, twigs were sampled only in the drought–lethal treatment during the last phase of dehydration, wherein ψ reached low values and needles were too desiccated to provide a trustful base for measurements. We measured ψ until values of < -7 MPa were reached. Based on our vulnerability curves (Figure S2 available as Supplementary data at *Tree Physiology* Online), we considered the trees dead at this stage. Daily means presented in the results section include a minimum sample size of three for the drought and two for the control treatments, with higher sample sizes for most days.

Leaf gas exchange

Midday leaf gas exchange, including stomatal conductance g_s (mmol m^{-2} s^{-1}), transpiration E (mmol m^{-2} s^{-1}) and net photosynthesis A_{net} (μmol m^{-2} s^{-1}), was measured using the portable LI-COR 6800 system (LI-COR Biosciences, Lincoln, NE, USA) on 10 specific days on the same needle cohorts for each species, covering different stages in the drought–recovery cycles (control $n = 3$, drought–recovery $n = 3 - 5$, drought–lethal $n = 3 - 5$). In the case of *P. sylvestris*, 10 needles were formed to a flat surface and enclosed in a leaf cuvette (2 cm^2). In the case of *L. decidua*, we enclosed one needle fascicle. Ambient cuvette parameters were kept constant, including a photosynthetic photon flux density of 2000 μmol m^{-2} s^{-1}, a CO_2 concentration of 410 p.p.m., a 10,000 r.p.m. fan speed, air temperature of 25°C and relative humidity of 50%. Due to stable VPD during the experiment (Figure S1 available as Supplementary data at *Tree Physiology* Online), g_s and E dynamics did not differ substantially (Figure S3 available as Supplementary data at *Tree Physiology* Online), so transpiration is not individually discussed in this work.

Vulnerability curves

We conducted Cavitron measurements (Cochard 2002) on the control seedlings ($n = 4$ per species) after the experiment. Stem samples were cut and directly re-cut under water, wrapped in cling film, enclosed in a cooling bag and transported to a laboratory at the University Innsbruck. Prior measurements, we completely removed the bark underwater, and samples were re-cut again on both ends to a length of 28 cm to fit into a custom-build rotor placed in a centrifuge (Sorvall RC-5; Thermo Fisher Scientific, Waltham, MA, USA) following the methods from Beikircher et al. (2010). We determined the percentage loss of conductance (PLC) by measuring the decrease in hydraulic conductivity while we reduced step-wise the rotational speed to increase the xylem pressure. PLC was calculated as

$$\mathrm{PLC} = 100 \cdot \frac{1 - k_t}{k_i}, \quad (1)$$

where k_i is the initial hydraulic conductance and k_t is the hydraulic conductance at the respective xylem pressure.

Dendrometer measurements

A total number of 13 trees per species (control $n = 3$, drought–recovery $n = 5$, drought–lethal $n = 5$) were equipped with dendrometers (Ecomatik Diameter Dendrometers, Type DD-S and DD-S1, 10-min frequency, 1.5 μm resolution) to capture relative variations in stem diameter. Before the sensor

installation (Figure S4 available as Supplementary data at *Tree Physiology* Online), we removed the most outer dead layers of the bark and measured the initial stem diameters per tree with a calliper to calculate absolute diameter changes from the dendrometer records.

One of the *P. sylvestris* drought–recovery trees equipped with a dendrometer showed an unexpectedly weak TWD–recovery after the final rewetting. As we cannot exclude a secondary pathogen infestation we excluded this seedling from further analysis.

Tree water deficit

We derived the TWD from the continuous high-resolution stem diameter variations as follows:

$$\mathrm{TWD} = d_{max} - d, \tag{2}$$

where d is the current absolute stem diameter and d_{max} is the maximum diameter measured for an individual tree in the past, which sets the theoretical maximum diameter under conditions of fully hydrated tissues. We apply the zero-growth concept, assuming that growth cannot occur during periods of stem contraction (Zweifel et al. 2016, Dietrich et al. 2018). In addition, we calculated a normalized TWD for treatment means:

$$\mathrm{TWD}_{norm} = \frac{\mathrm{TWD}}{\mathrm{TWD}_{max}}, \tag{3}$$

where TWD_{max} is the highest TWD occurring for drought–lethal trees at the end of the experiment.

Statistical analyses

We performed data processing, visualization and statistical analysis with the programming language R, version 4.2.2 (R Core Team 2022). The significance of treatment and species differences was evaluated using a linear mixed model likelihood ratio test (*'lme'* package; Bates et al. (2015)). All results presented are treatment means with standard error (SE). To derive the matching TWD with midday ψ and g_s in the shown relationships, we averaged the TWD of all dendrometer-equipped trees between 1 and 4 p.m. on the corresponding days (midday TWD). Besides, we derived pre-dawn TWD, averaged from 3 to 4 a.m. Note that the g_s and ψ treatment means also include measurements on trees not equipped with dendrometers to reduce destructive harvest per tree. Data for individual trees is depicted in the supplementary material (Figure S5 available as Supplementary data at *Tree Physiology* Online). Regression fits were produced with the *nls()* function, and the 95% confidence intervals for all regression parameters and regression curves were estimated via bootstrapping. For the relation between TWD_{norm} and ψ, we used the following sigmoidal regression:

$$\mathrm{TWD}_{norm}(\psi) = \frac{A}{1 + e^{-b \cdot (\psi + c)}}, \tag{4}$$

where e is the Euler function and the parameters A, b and c determine the asymptotic behavior, steepness and inflection point (indicating 50% of water depletion). While in the literature, this approach is usually applied (e.g. Dietrich et al. 2018), its inversion is mathematically complex, particularly at the assumed plateaus where multiple ψ values belong to the same TWD, which hinders ψ retrieval directly from TWD measurements. Therefore, in a second approach, we reversed axes, separated TWD_{norm}–ψ data into three 'slope groups' and fitted linear curves ($\psi(TWD_{norm}) = a \cdot TWD_{norm} + C$). We defined the cross-sections of the regression lines as thresholds for phase changes. For the relationship between g_s and TWD_{norm}, we chose an exponential approach:

$$g_s(\mathrm{TWD}_{norm}) = a \cdot e^{-b \cdot \mathrm{TWD}_{norm}} + C, \tag{5}$$

where the parameter a defines the vertical scaling, b the bending and C and the vertical offset of the function. Equation (5) was further used to retrieve thresholds for stomatal closure, in expression the TWD_{norm} at g_s equaling 5 and 50% (TWD_{g5}, TWD_{g50}) of the g_s control mean. Similarly, ψ_{g5} and ψ_{g50} (equaling the concept of G_{c50} in Peters et al. 2023) thresholds were retrieved from sigmoidal g_s-ψ relationships ($g_{norm}(\psi) = 1/(1 + exp(-a * (\psi + b)))$).

The software package *'fitplc'* (Duursma and Choat 2017) was applied to create vulnerability curves from the Cavitron measurements. We used sigmoidal regressions and determined ψ values introducing a PLC of 12, 50 and 88% (P_{12}, P_{50}, P_{88}), which function as key hydraulic thresholds (Urli et al. 2013, Dorji et al. 2024).

Results

Vulnerability to drought

The hydraulic vulnerability curves of both species, *L. decidua* and *P. sylvestris*, indicate similar P_{50} values of −3.16 and −3.11 MPa (Table 1a) and thus comparable drought susceptibility, which is in agreement with ranges determined for mature trees in Peters et al. (2023). However, the curve for *L. decidua* is steeper, corresponding to a faster rate of conductance loss per decrease of ψ (Figure S2 available as Supplementary data at *Tree Physiology* Online). Besides, in the case of *P. sylvestris* ψ values corresponding to halfway and fully closed stomata (ψ_{g50}, ψ_{g5}) are higher, and the slope of the response curve at ψ_{g50}—a measure for isohydricity (Peters et al. 2023)—is steeper, indicating a stricter stomatal control (Table 1b, Figure S6 available as Supplementary data at *Tree Physiology* Online).

Tree water status during drought recovery cycles

Changes in SWC affected both ψ and TWD (Figure 2, Table 2). During D1, ψ exhibited a slight yet significant decrease compared with control conditions ($P \leq 0.01$). Concurrently, stem diameter variations displayed increased diurnal amplitudes, particularly pronounced in *L. decidua*. By the end of D1, TWD did not fully vanish during nighttime and started to accumulate. After stress release, TWD and ψ both returned to control levels. In the more prolonged drought period D2, ψ levels reached −3.0 ± 0.2 MPa and −2.7 ± 0.2 MPa for *L. decidua* and *P. sylvestris*, respectively. Initially, TWD exhibited an increased diurnal cycle again, but after approximately 2 weeks, stem shrinkage continued without any diameter expansion during the night. By the end of D2, TWD levels reached 1.3 ± 0.1 mm for *L. decidua* and 1.6 ± 0.2 mm for *P. sylvestris*, translating to a relative shrinkage of 12.5 ± 0.6 and 10.5 ± 1.0 % and a TWD_{norm}

Table 2. Water status and gas exchange variables during a drought and recovery experiment conducted on potted seedlings of *L. decidua* (L) and *P. sylvestris* (P) under controlled conditions. Depicted are water potential (ψ), tree water deficit (TWD), soil water content (SWC), stomatal conductance (g_s) and net photosynthesis (A_{net}). The values correspond to Figures 2 and 4 and indicate the mean ± SE of the control treatment across the experiment, as well as treatment means ± SE of the drought treatment at the end of the first and second drought phase (D1 and D2) and of the drought–lethal treatment at the end of the experiment. The last two columns correspond to the time re-watered trees required to fully recover to pre-stress levels after D1 and D2, respectively.

Parameter	Species	Mean control	End D1	End D2	End drought–lethal	Recovery D1 (days)	Recovery D2 (days)
ψ [−MPa]	L	1.1 ± 0.02	1.2 ± 0.1	3.0 ± 0.2	7.0 ± 0	< 3	< 1
	P	0.6 ± 0.02	1.0 ± 0.1	2.7 ± 0.2	6.5 ± 0.5	< 3	< 1
TWD [mm]	L	0.01 ± 0.0002	0.3 ± 0.03	1.3 ± 0.1	1.8 ± 0.1	0	8 ± 1
	P	0.04 ± 0.0002	0.2 ± 0.04	1.6 ± 0.2	2.1 ± 0.2	0	9 ± 1
TWD [%]	L	0.1 ± 0.001	2.7 ± 0.2	12.5 ± 0.6	16.4 ± 0.4		
	P	0.2 ± 0.001	1.3 ± 0.2	10.5 ± 1.0	14.3 ± 0.8		
SWC [%]	L	33.6 ± 0.3	18.9 ± 1.8	2.8 ± 0.6	0.1 ± 0.1	0	0
	P	33.5 ± 0.2	17.8 ± 1.6	1.9 ± 0.7	0.2 ± 0.2	0	0
g_s [$\frac{\text{mmol}}{\text{m}^2\,\text{s}}$]	L	104 ± 7	12 ± 1	3 ± 0.4	3 ± 2	< 3	20 ± 3
	P	76 ± 5	10 ± 3	3 ± 0.3	3 ± 0.5	< 3	10 ± 3
A_{net} [$\frac{\mu\text{mol}}{\text{m}^2\,\text{s}}$]	L	5.4 ± 0.3	1.9 ± 0.2	0.0 ± 0.04	-0.1 ± 0.03	< 3	12 ± 3
	P	6.0 ± 0.3	1.3 ± 0.3	0.0 ± 0.04	-0.1 ± 0.05	< 3	6 ± 3

of 0.76 and 0.73. Upon rewetting, plants of the drought–recovery treatment showed an instantaneous recovery of ψ. In contrast, TWD decreased rapidly after stress release but did not fully return to control values ($P < 0.01$). For *L. decidua*, approximately 85 ± 3% of the diameter shrinkage was reversed within 1 day, while for *P. sylvestris*, this value was 80 ± 2%. Subsequently, both species resumed daily stem diameter variations gradually decreasing TWD. Ultimately, TWD returned to the control values after 8 days for *L. decidua* and after 9 days for *P. sylvestris*.

Relationship between TWD and ψ

We found a strong relationship between TWD and ψ persisting across all drought conditions until lethal dehydration in both *L. decidua* and *P. sylvestris*. It can be effectively characterized by a single species-specific sigmoidal fit (Figure 3a and b; pseudo-R^2 of 0.97 for both species). To better assess the possibility of using TWD as a predictor for ψ we replotted the data with reversed axes (Figure 3c and d) and found three distinct phases. Phase (I) shows an initial decrease in ψ with a low TWD response, (II) a steep linear relation indicating decreasing ψ with increasing TWD and (III) a less pronounced increase in TWD with further decreasing ψ. The first change of phases occurs at a normalized TWD of 0.02 for *L. decidua* and 0.04 for *P. sylvestris*, respectively, with corresponding ψ close to ψ_{g50} (ψ at g_s = 50% of control). The second shift appears at a TWD_{norm} of 0.74 and 0.81, corresponding to ψ values of −3.0 MPa and −2.9 MPa (in between P_{12} and P_{50}). The R^2 is lowest with 0.64 in phase (I) for *L. decidua*, while in all other cases R^2 is ≥ 0.88 for both species.

However, the responses of the drought–recovery treatment (green triangles in Figure 3a and b) could not adequately be represented by the ψ–TWD relationship as observed during continuous drought development. Upon rewetting after D2, immediate recovered ψ values correspond to TWD persisting at levels higher than anticipated by the sigmoidal fit. In contrast, rewetting after D1 did not exhibit such prolonged effects on TWD.

Taking a closer look at species-specific TWD–ψ responses, we found slight differences in timing and depletion rates. Specifically, TWD accumulates at lower ψ levels for *L. decidua* compared with *P. sylvestris*. The point at which 50% of water is depleted (c parameter in the sigmoidal fit) occurred significantly later for *L. decidua* compared with *P. sylvestris*: −2.3 ± 0.1 MPa versus −2.0 ± 0.1 MPa ($P < 0.01$). Additionally, *L. decidua* exhibited a higher shrinkage rate per MPa ψ (b parameter in the sigmoidal fit, $P < 0.01$).

Leaf gas exchange during drought–recovery cycles

Leaf gas exchange was highly sensitive to both drought and rewetting conditions (Figure 4, Table 2). At the end of D1, ψ reached 1.2 ± 0.1 MPa for *L. decidua* and 1.0 ± 0.1 MPa for *P. sylvestris*. Accordingly, g_s was reduced significantly ($P < 0.01$) to 11.5 and 13.3% of control values, respectively, while A_{net} dropped to 35.2 and 21.7%. The ψ_{g5} of full stomatal closure was reached in the first half of D2. During the remaining drought period, g_s remained at its minimum and A_{net} approached zero. Leaf gas exchange fluxes quickly returned to control values after D1 but required time for full recovery following D2 (Table 2). In particular, g_s recovery after D2 took approximately 20 ± 3 days for *L. decidua* and 10 ± 3 days for *P. sylvestris*. Similarly, the recovery period for A_{net} was approximately 12 ± 3 in *L. decidua* and 6 ± 3 days *in P. sylvestris*. Hence, the gas exchange of *P. sylvestris* tended to recover faster compared with *L. decidua*, with g_s recovering generally slower than A_{net} in both species.

Relationship between TWD and g_s

We found a strong exponential relationship between g_s and both the midday (Figure 5a and b) and pre-dawn TWD (Figure 5c and d) during dehydration. Corresponding pseudo-R^2 values are 0.87 in both cases for *L. decidua* and 0.77 and 0.81 for midday and pre-dawn TWD, respectively, for *P. sylvestris*. Small increases in TWD resulted in drastic decreases in gas exchange, which appeared more pronounced for pre-dawn than for midday TWD, highlighting the sensitivity of g_s to water deficit. While midday TWD allows estimations of partial stomatal closure, the pre-dawn TWD signal provided a clearer response at full stomatal closure, indicated by a phase shift at TWD >0. In more detail, at a midday TWD_{norm} of 0.06 for *L. decidua* and 0.08 for *P. sylvestris* 50% stomatal closure was reached (md-TWD_{g50}), shortly after the first

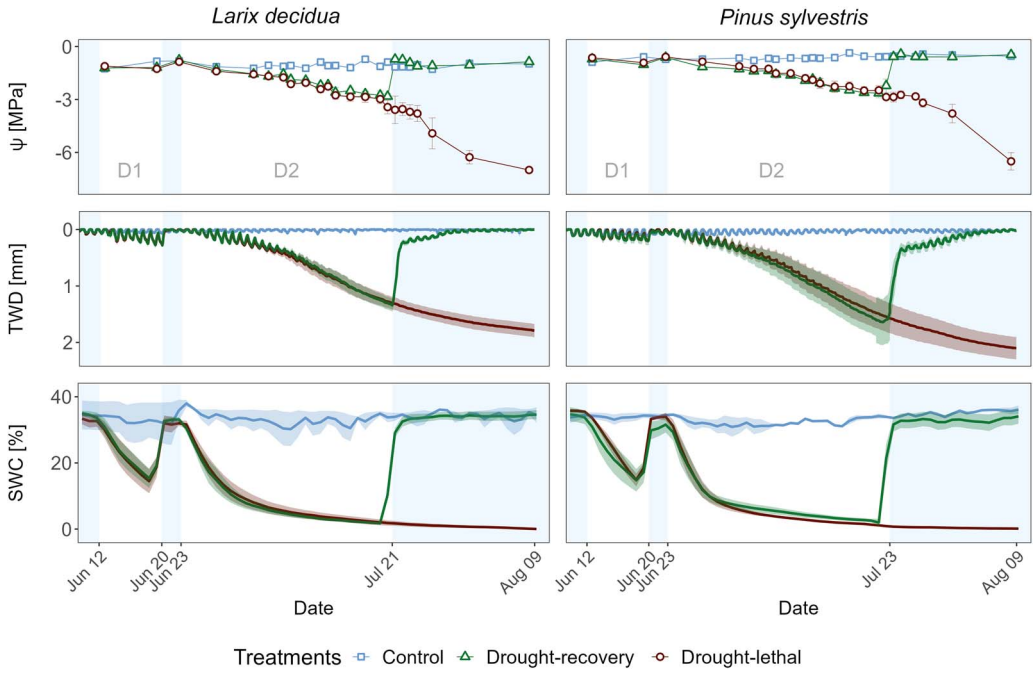

Figure 2. Temporal dynamics of water relations during a drought and recovery experiment conducted on potted seedlings (*L. decidua, P. sylvestris*) under controlled conditions. Depicted are water potential (ψ), tree water deficit (TWD) and soil water content (SWC) as treatment means ± SE. The two drought phases are marked as D1 and D2, and the recovery phases are illustrated with a blue background. In the final recovery phase, the drought treatment was split equally and only drought–recovery seedlings were re-watered, while drought–lethal trees were fully dehydrated.

shift in the TWD–ψ relation and in a range where pre-dawn TWD is still 0. Stomatal closure became apparent at midday TWD values of 0.23 and 0.25 for *L. decidua* and *P. sylvestris*, respectively, corresponding to pre-dawn TWD values of only 0.02 and 0.07 (md- and pd-TWD_{g5}).

Due to different recovery behaviors of TWD and g_s, the drought–recovery treatment following the final rewetting was slightly outside the expectation of the exponential curves for both species. However, we found species-specific differences. For *L. decidua*, g_s during drought–recovery was partly lower than anticipated by the regression curve due to a delayed gas exchange recovery. Conversely, for *P. sylvestris*, g_s deviated from the curve with values higher than expected, indicating a delay in TWD recovery. While the recovery of g_s and TWD showed similar trends, it differed in timing. g_s exhibited a gradual recovery, whereas TWD initially showed a rapid response followed by a gradual decrease.

Discussion

Our data confirm strong relationships between ψ and TWD, as well as g_s and TWD. However, these relationships became unstable during recovery after severe drought. While dendrometer-based TWD measurements show promise for predicting ψ (Dietrich et al. 2018) and can serve as a drought stress indicator, caution is required when including periods of drought recovery in the analysis.

How does TWD develop with decreasing ψ?

The relationship between TWD and ψ was robust for both investigated tree species, including severe and lethal drought stress, but not during the recovery phase after D2 (see section 4.2). Both species showed similar TWD patterns, supporting previous studies indicating minor differences in drought susceptibility (Dulamsuren et al. 2019, Feng et al. 2021). Nevertheless, we found species-specific disparities. *L. decidua* exhibited a weaker stomatal control (Peters et al. 2023) and responded more anisohydric than *P. sylvestris* (Oberhuber et al. 2015). Additionally, *L. decidua* demonstrated a greater rate of shrinkage per ψ decrease during dehydration, aligning with expectations of high transpiration rates even under dry conditions (Leštianska et al. 2020).

We observed shifts in the TWD–ψ relationship with increasing water shortage, representable by either a single sigmoidal curve or distinct linear fits. Sigmoidal regressions were proposed by Dietrich et al. (2018) and the authors expect a saturation of TWD at the lowest ψ they have measured (about −2.5 MPa for *L. decidua* and −1.8 MPa for *P. sylvestris*). In contrast, our data suggest that TWD has not reached half its maximum at this ψ. Besides an overall high correlation, the sigmoidal fit fails to capture the development under the lowest ψ levels for our data. After expected tree death, as suggested by ψ measurements, it seems that the remaining water availability in elastic tissues did not lead to an asymptotic TWD saturation but a continued shrinkage, as demonstrated in phase (III) (Figure 3 c and d) and supported by similar findings of Andriantelomanana et al. (2024) for *Populus tremula*. This also induces difficulties selecting TWD_{max}, which is crucial for normalization of the TWD signal (see section 4.4). Linear TWD–ψ relationships were also found for the tropical species *Callitris intratropica* (Drew et al. 2011) and the temperate species *Juglans regia* (Cochard et al. 2001), *Picea abies* and *Larix decidua* (Oberhuber et al. 2015). However, none of these studies captured severe drought stress and slope shifts in the TWD–ψ relationship were consequently not present. Overall, the linear approach appears more realistic and applicable. While the sigmoidal method requires a complex inversion for ψ retrievals, the linear procedure allows direct predictions.

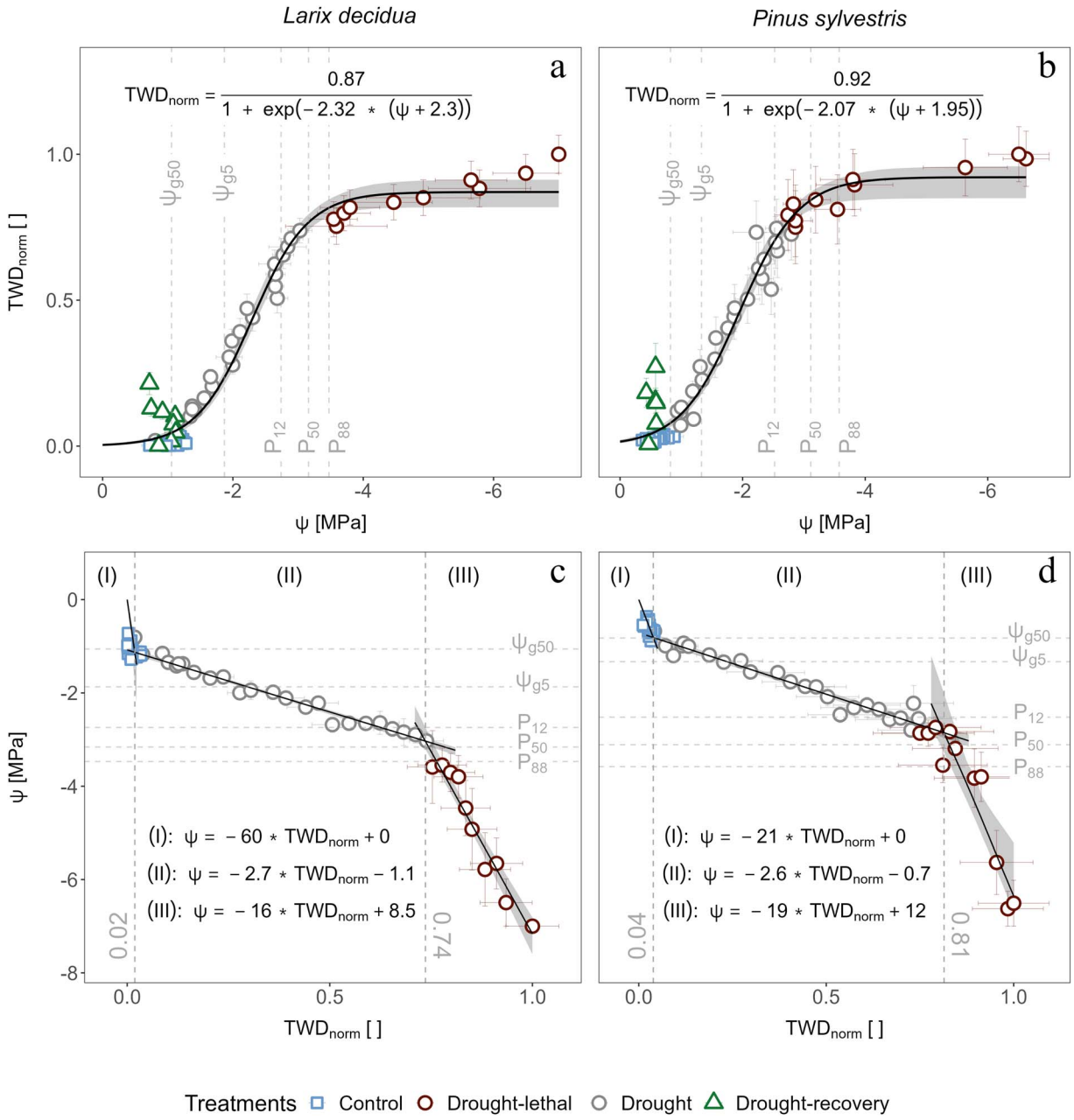

Figure 3. Relationship between midday water potential (ψ) and normalized tree water deficit (TWD_{norm}) during a drought and recovery experiment conducted on potted seedlings (*L. decidua*, *P. sylvestris*) under controlled conditions. In the upper row (a, b), we applied a sigmoidal fit with ψ as the predictor variable. In the bottom row (c, d), we reversed axes and split the data into three distinct phases with linear regressions (excluding the drought–recovery treatment). Data are treatment means ± SE. The TWD was derived from measurements between 1 and 4 p.m. corresponding to the ψ measurements. Normalized TWD was derived relative to the largest averaged TWD in the drought–lethal trees. Shaded areas depict the 95% confidence intervals of the fitted regressions.

Although defining additional inclination points may be a practical limitation, these inclination points could serve as valuable stress-severity thresholds. However, caution is required when extending regression curves beyond their calibrated range. For instance, Vergeynst et al. (2015) suggest extrapolating a single linear ψ–TWD regression fit for continuous ψ determination. With a slope change appearing at the onset of hydraulic damage, as our data suggest, such an extrapolation will lead to errors under severe drought stress (here in phase (III)). Also, predicting ψ under near-zero TWD is difficult despite a linear correlation, while in phases (II) and (III), TWD becomes a better predictor as dehydration accumulates.

We propose that the two slope changes in the TWD–ψ relationship (Figure 3c and d) can serve as thresholds for the onset of initial drought stress and the loss of instant recovery potential. While often a subsequent release of water from elastic and inelastic tissues during dehydration is proposed, Lauriks et al. (2022) suggest an overlapping, and Andriantelomanana et al. (2024) a fully simultaneous succession. Our results support partially overlapped water release from elastic and inelastic tissues and distinct phases indicating different drought severity and recovery potential. For phase (I), we hypothesize a parallel release of apoplastic and symplastic water with apparent but low volume loss. At this stage, the

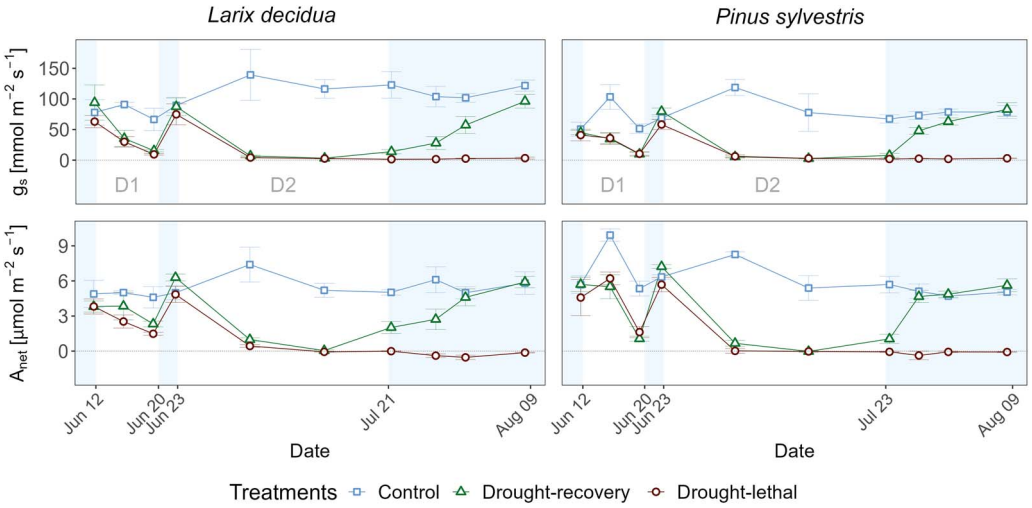

Figure 4. Temporal dynamics of leaf gas exchange in the course of a drought and recovery experiment conducted on potted seedlings (*L. decidua, P. sylvestris*) under controlled conditions. Depicted are stomatal conductance (g_s) and net photosynthesis (A_{net}) as treatment means ± SE. The two drought phases are marked as D1 and D2, and the recovery phases are illustrated with a blue background. In the final recovery phase, the drought treatment was split equally and only drought–recovery seedlings were re-watered, while drought–lethal trees were fully dehydrated.

TWD vanishes at night, indicating no soil water limitation. The shift to phase (II) seems to be triggered by stomatal closure, as it occurs around ψ_{g50}. Further dehydration results in complete stomatal closure within the phase. Here, accumulation of TWD due to water release purely stems from elastic tissues, leading to the highest depletion rate. In contrast to the observation of Andriantelomanana et al. (2024), our data suggest no water release from inelastic tissues until the end of the phase according to the determined vulnerability curves and measured ψ. We assume that the second shift in slope corresponds to the onset of hydraulic damages as it occurs between P_{12} and P_{50}. In phase (III), P_{88} is accompanied by less rapid but nonetheless persistent shrinkage, indicating further release of symplastic water, joined by water release from embolized xylem conduits. Mantova et al. (2022) argue that cavitation events trigger the collapse of living cells, i.e. cell necrosis due to mechanical or oxidative stress. In particular, the loss of meristematic cells is critical since they play a crucial role in the survival and recovery of trees. While embolized xylem conduits are lost, secondary growth building new xylem can improve conductance. However, this requires surviving meristematic cells with a functional water supply (Mantova et al. 2022). Water released by xylem embolism may be used to sustain hydration of elastic tissues (Skelton 2020), and hence delaying cell collapse (Knipfer et al. 2019, Lamacque et al. 2020). Further shrinkage in phase (III) suggests increasing PLC and meristematic cell loss, leading to longer recovery after stress release. At a certain threshold, the recovery potential may be lost completely, resulting in tree death (Lamacque et al. 2020, Andriantelomanana et al. 2024).

Is the relationship between TWD and ψ impacted by stress release?

Since physiological processes recover at different rates after severe drought (Ruehr et al. 2019, Rehschuh et al. 2020), we expected a changed TWD–ψ relationship during recovery. While the severe drought phase D2 caused changes, the mild drought conditions in D1 had negligible impact. During D1, the highest occurring TWD was within the early part of phase (II), and stress release led to an instantaneous recovery of all physiological parameters, shifting the TWD–ψ relationship back to its initial stage. In contrast, at the end of D2, *P. sylvestris* trees were within the latter part of phase (II) and *L. decidua* trees in the early part of phase (III). Despite the rapid increase of ψ to levels similar to controls, TWD did not fully recover for several days in both species. Interestingly, the diameter increase showed similarities to a capacitor recharge curve, and further investigations might enable valuable insights into tree-water relations from TWD recovery, such as capacitance determination. In the TWD–ψ relationship, we observed a recovery hysteresis effect. The drought–recovery treatment deviated from the curve (Figure 3a and b) but gradually approached it again while TWD recovered back to control values. Hence, during this phase, the relationship does not hold. The distinct recovery behavior after D1 and D2 further supports our argument that the trees lose their potential for instantaneous recovery at the shift from phase (II) to phase (III).

However, whether the incompletely recovered stem diameter after rewetting still indicates a water deficit is arguable. By definition, TWD is greater zero if the current diameter is smaller than the maximum diameter in the past (see Eq. (2)). On the other hand, TWD is supposed to reflect the condition where elastic tissues are not fully hydrated and, consequently, not at their maximum volume. The sharp diameter increase after stress release stopped after approximately one day without full recovery to pre-stress conditions, eventually caused by an impairment of the xylem-phloem connection increasing radial resistance (Steppe et al. 2006, Salomón et al. 2017). Another explanation might be the collapse of elastic cells, which can not rehydrate afterwards (Lamacque et al. 2020, Fortunel et al. 2023). In this case, the disparity in diameter observed one day after stress release would indicate accumulated cell damage rather than a persistent water deficit.

Thus, the incomplete recovery of stem diameter after stress release may be a proxy for assessing cell damage and, consequently, recovery potential or even mortality risk. Previous studies have identified specific thresholds for TWD beyond which mortality occurs. *Lavandula* seedlings perished

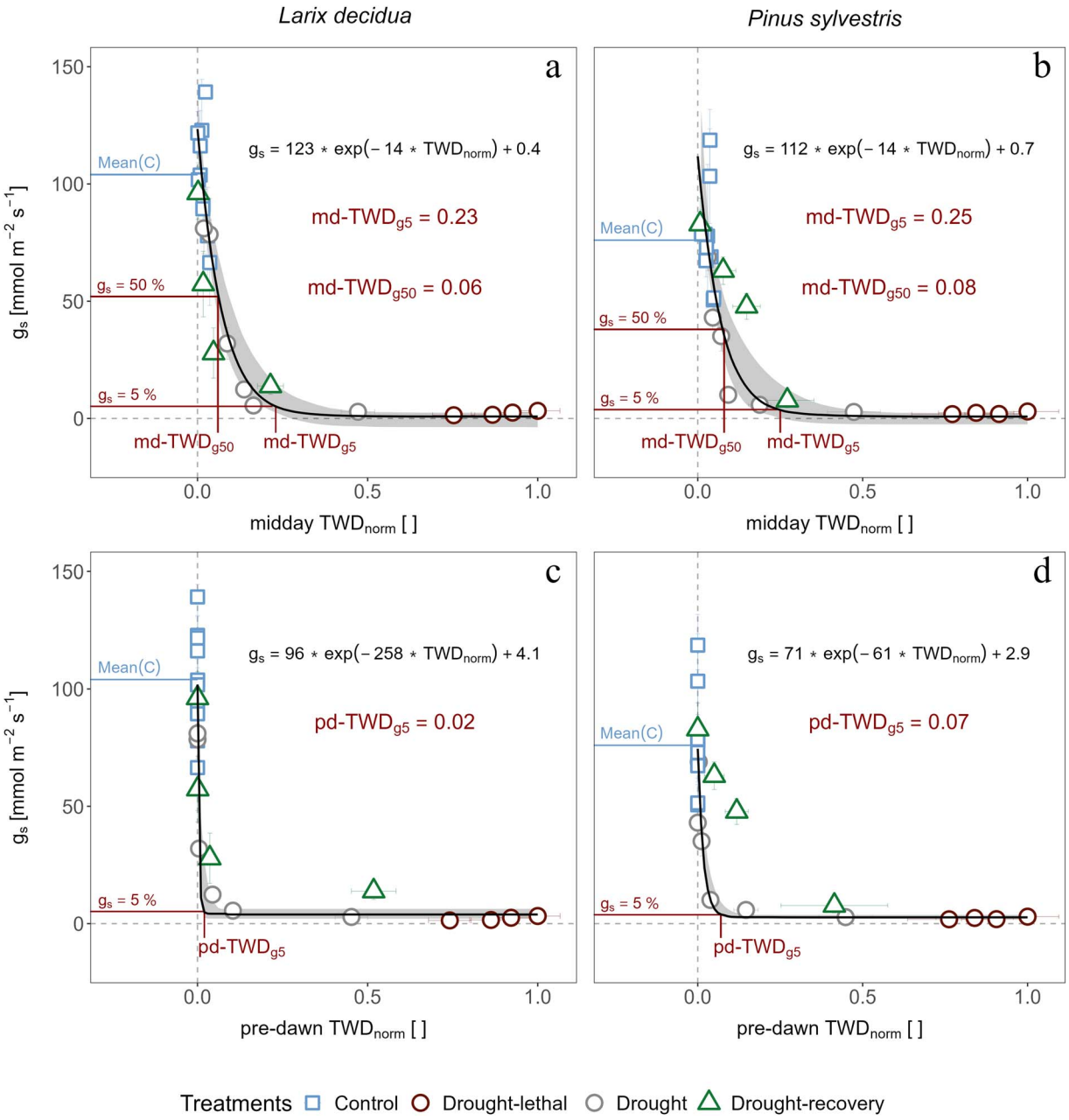

Figure 5. Relationship between midday leaf-level stomatal conductance (g_s) and normalized tree water deficit (TWD_{norm}) during a drought and recovery experiment conducted on potted seedlings (*L. decidua*, *P. sylvestris*) under controlled conditions. In (a, b), g_s is related to midday (md) TWD, derived from measurements between 1 and 4 p.m. corresponding to the g_s measurements. In (c, d), g_s is related to pre-dawn (pd) TWD, derived from measurements between 3 and 4 a.m. We applied exponential fits (black) neglecting the drought–recovery data points with the shaded area indicating the 95% confidence interval of the curve. Additionally, the TWD_{norm} at g_s equaling 5% (a–d; TWD_{g5}) and 50% (a–b; TWD_{g50}) of the control mean (Mean(C)) was determined. Data are treatment means ± SE. Normalized TWD was derived relative to the largest averaged TWD in the drought–lethal trees.

once they reached a stem shrinkage of approximately 21% (Lamacque et al. 2020), while *Populus tremula* seedlings succumbed at values ranging from 7 to 12%, depending on growth conditions (Andriantelomanana et al. 2024). In our study, the maximum stem shrinkage reached during D2 was 12.5 ± 0.6% for *L. decidua* and 10.5 ± 1.0% for *P. sylvestris*. Although none of the trees died, they all required a prolonged recovery time and can be supposed to have experienced damaged tissue. In *L. decidua*, 85% of the diameter shrinkage reversed after stress release, which may indicate that roughly 15% of living parenchyma or meristematic cells were irreversibly damaged. For *P. sylvestris* this value corresponds to 20%. Despite higher ψ_{min} values before rewetting compared with *L. decidua* and similar P_{50}, *P. sylvestris* exhibited higher tissue damage susceptibility. Notably, damage was not directly quantified in this study, and the exact cause of the incomplete diameter recovery is debatable. Further investigations of partial TWD recovery upon various stress levels and TWD thresholds for mortality may yield promising metrics enabling drought damage predictions, especially if they include in-situ embolism and cell collapse quantification.

How are TWD and gas exchange related?

The exponential decline of g_s with increasing TWD is consistent with findings from two *Lavandula* species (Lamacque et al. 2020). While the initial decrease in ψ does not directly limit g_s (Rehschuh et al. 2020), the first increase in TWD already signified drought stress, triggering partial stomatal closure and subsequent declines in gas exchange. Once TWD did not fully recover during the night, leading to a pre-dawn TWD greater than 0, stomata were closed or nearly closed the following midday—a stress signal directly applicable to field conditions. However, a direct quantitative prediction of g_s appears challenging due to the sensitive response between g_s and TWD. Alternatively, TWD could be used to estimate ψ, facilitating a more straightforward prediction of the gas exchange rates with hydraulic models (Anderegg et al. 2017, Eller et al. 2018). Besides quantifying g_s relations, correlations between TWD and transpiration might reveal interesting insights, especially if one considers canopy-level transpiration as a measure of whole tree water loss under variable VPD (Peters et al. 2023).

Upon stress release after D2, we observed hysteresis effects in the g_s–TWD relationships due to asynchronous TWD and gas exchange recovery. The restoration of pre-stress levels seems to depend on tissue damage and recovery strategies. In general, the recovery of stomatal conductance is complex and relies on species-specific factors such as genotype, abscisic acid concentration, hydraulic resistance and transpiration rates (Buckley 2019). In the case of *L. decidua*, a higher percentage of shrinkage was reversed directly after stress release, resulting in a slightly faster TWD recovery. *Pinus sylvestris* showed less immediate TWD recovery but a faster recovery in g_s and the carbon assimilation rate A_{net}. This differential recovery may indicate distinct priorities, with *P. sylvestris* emphasizing gas exchange recovery. In contrast to D2, the mild drought D1 did not exhibit changes in the g_s–TWD relationship, aligning with the observation that gas exchange only requires prolonged recovery after hydraulic impairments occurred (Skelton et al. 2017).

The thresholds at which stomata close in response to increasing TWD are likely species specific (Lamacque et al. 2020, Andriantelomanana et al. 2024) and reflect individual water-use strategies. Trees rely on internal water reservoirs during drought, resulting in varying degrees of stomatal closure depending on the species' tendency to limit water loss. However, in our study, both *L. decidua* and *P. sylvestris* exhibited nearly identical g_s–TWD relationships, despite differences in water use strategies (Oberhuber et al. 2015, Martín-Gómez et al. 2023) and different ψ_{g50} and ψ_{g5} values. Consequently, stomatal closure developed at similar TWD thresholds. These thresholds likely depend on stomatal density, leaf traits and the possibility of reducing internal conductivity by non-stomatal effects. For example, *Lavandula* species fully close stomata at a stem shrinkage of ≈5% (Lamacque et al. 2020), while in our case md-TWD_{g5} translates to values of approximately 2% for *L. decidua* and 1.7% for *P. sylvestris*, indicating a more sensitive stomatal response. *Populus tremula* reacts even faster, with full stomatal closure reported at the onset of midday TWD accumulation (Andriantelomanana et al. 2024). Investigating such responses offers a promising approach to assessing water-use strategies. Besides, TWD thresholds for stomatal closure could serve as warning signals in field conditions. Practically, monitoring the occurrence of pre-dawn TWD might be a simple and directly applicable measure to predict stomatal closure. Applying midday TWD_{g50} and TWD_{g5} appears to provide more detailed insights into the degree of stomatal opening. However, transferring these thresholds (and ψ–TWD relations) requires normalization of TWD signals, a challenge still limiting practical use.

The challenge of normalizing TWD

A significant challenge in applying TWD relationships in field conditions is the normalization with TWD_{max}, especially when lethal conditions are not captured by measurements. In our study, we defined TWD_{max} as the mean maximum TWD of drought–lethal trees at the end of the experiment. However, post-mortem shrinkage complicates this choice, as defining TWD_{max} at a different time would alter thresholds and relationship functions. Additionally, transferring TWD_{max} to different tree sizes and environmental conditions requires careful consideration, given that tissue shrinkage depends on factors such as bark-to-xylem ratio, wood density, elastic modulus and growth conditions (Andriantelomanana et al. 2024). For instance, *P. sylvestris* exhibited greater absolute shrinkage than *L. decidua*, but the latter showed a larger relative shrinkage (Table 2), possibly indicating more water storage in elastic cells, supported by a thicker bark and a lower bark-to-xylem ratio (0.48 vs 0.25; Figure S7 available as Supplementary data at *Tree Physiology* Online). Future research should aim for a more stable and transferable normalization, e.g. by differentiating between bark and xylem shrinkage, or by experimenting with different normalization variables such as maximum daily shrinkage (Peters et al. 2023).

Conclusions

Dendrometer-derived TWD provides direct insights into the water dynamics of individual trees by enabling continuous ψ determination, the assessment of stomatal closure and the application of tree drought stress thresholds. However, the normalization of the TWD data remains a challenge and affects transferability. Additionally, recovery phases following severe droughts can alter the TWD relationships to ψ and g_s. On the positive side, the incomplete diameter recovery after stress release provides an opportunity to quantify drought-induced damage and estimate recovery times. Dendrometer networks, capable of collecting data from numerous trees, allow the evaluation of tree functionality at larger scales. These networks could serve as early warning systems, detecting initial drought onset as well as severe drought conditions. A persisting TWD not refilled during the night is a clear drought stress signal, accompanied by drastically reduced midday leaf gas exchange. Further TWD accumulation can then hint towards critical damage to tree functionality and, ultimately, the risk of tree mortality. Identifying susceptible species and locations could guide mitigation efforts and appropriate management actions. Applications extend to urban environments for tree watering practices and forest ecosystems to support comprehensive monitoring efforts.

Acknowledgments

We thank Prof. Stefan Mayr from the University of Innsbruck for the possibility of using the Cavitron infrastructure in his lab.

Supplementary data

Supplementary data are available at *Tree Physiology* Online.

Authors' contributions

Y.Z., N.K.R. and R.G. designed the experiment. Y.Z., supported by F.A. and T.K., performed the measurements. Y.Z. analyzed the data and wrote the manuscript, with input and approval from all authors.

Funding

The study has been funded through the Helmholtz Initiative and Networking fund (W2/W3-156).

Conflict of interest

None declared.

Data availability

The data that underlie this study are available upon request.

References

Allen CD, Macalady AK, Chenchouni H et al. (2010) A global overview of drought and heat-induced tree mortality reveals emerging climate change risks for forests. For Ecol Manage 259:660–684. https://doi.org/10.1016/j.foreco.2009.09.001.

Anderegg WR, Wolf A, Arango-Velez A et al. (2017) Plant water potential improves prediction of empirical stomatal models. PloS One 12:e0185481. https://doi.org/10.1371/journal.pone.0185481.

Andriantelomanana T, Améglio T, Delzon S, Cochard H, Herbette S (2024) Unpacking the point of no return under drought in poplar: insight from stem diameter variation. New Phytol 242:466–478. https://doi.org/10.1111/nph.19615.

Bates D, Maechler M, Bolker B et al. (2015) Package 'lme4'. convergence 12:2. https://github.com/lme4/lme4/.

Beikircher B, Ameglio T, Cochard H, Mayr S (2010) Limitation of the Cavitron technique by conifer pit aspiration. J Exp Bot 61: 3385–3393. https://doi.org/10.1093/jxb/erq159.

Buckley TN (2019) How do stomata respond to water status? New Phytol 224:21–36. https://doi.org/10.1111/nph.15899.

Choat B, Jansen S, Brodribb TJ et al. (2012) Global convergence in the vulnerability of forests to drought. Nature 491:752–755. https://doi.org/10.1038/s41586-018-0240-x.

Choat B, Brodribb TJ, Brodersen CR, Duursma RA, López R, Medlyn BE (2018) Triggers of tree mortality under drought. Nature 558: 531–539. https://doi.org/10.1038/s41586-018-0240-x.

Cochard H (2002) A technique for measuring xylem hydraulic conductance under high negative pressures. Plant Cell Environ 25:815–819. https://doi.org/10.1046/j.1365-3040.2002.00863.x.

Cochard H, Forestier S, Améglio T (2001) A new validation of the Scholander pressure chamber technique based on stem diameter variations. J Exp Bot 52:1361–1365. https://doi.org/10.1093/jexbot/52.359.1361.

De Swaef T, De Schepper V, Vandegehuchte MW, Steppe K (2015) Stem diameter variations as a versatile research tool in ecophysiology. Tree Physiol 35:1047–1061. https://doi.org/10.1093/treephys/tpv080.

Dietrich L, Zweifel R, Kahmen A (2018) Daily stem diameter variations can predict the canopy water status of mature temperate trees. Tree Physiol 38:941–952. https://doi.org/10.1093/treephys/tpy023.

Dixon F (1915) Transpiration and the ascent of sap in plants. Nature 94:558–559.

Dorji Y, Isasa E, Pierick K, Cabral JS, Tobgay T, Annighöfer P, Schuldt B, Seidel D (2024) Insights into the relationship between hydraulic safety, hydraulic efficiency and tree structural complexity from terrestrial laser scanning and fractal analysis. Trees Struct Funct 38: 221–239. https://doi.org/10.1007/s00468-023-02479-1.

Drew DM, Richards AE, Downes GM, Cook GD, Baker P (2011) The development of seasonal tree water deficit in Callitris intratropica. Tree Physiol 31:953–964. https://doi.org/10.1093/treephys/tpr031.

Dulamsuren C, Abilova SB, Bektayeva M, Eldarov M, Schuldt B, Leuschner C, Hauck M (2019) Hydraulic architecture and vulnerability to drought-induced embolism in southern boreal tree species of inner Asia. Tree Physiol 39:463–473. https://doi.org/10.1093/treephys/tpy116.

Dunkleberger R, Sauchyn DJ, Vanderwel MC (2023) Using thermal imagery and changes in stem radius to assess water stress in two coniferous tree species. Agric For Meteorol 341:109686. https://doi.org/10.1016/j.agrformet.2023.109686.

Duursma RA, Choat B (2017) fitplc: an R package to fit hydraulic vulnerability curves. J Plant Hydraul 4:e002. https://doi.org/10.20870/jph.2017.e002.

Eller CB, Rowland L, Oliveira RS et al. (2018) Modelling tropical forest responses to drought and El Niño with a stomatal optimization model based on xylem hydraulics. Philos Trans R Soc Lond B Biol Sci 373:20170315. https://doi.org/10.1098/rstb.2017.0315.

Feng F, Losso A, Tyree M, Zhang S, Mayr S (2021) Cavitation fatigue in conifers: a study on eight European species. Plant Physiol 186: 1580–1590. https://doi.org/10.1093/plphys/kiab170.

Fortunel C, Stahl C, Coste S et al. (2023) Thresholds for persistent leaf photochemical damage predict plant drought resilience in a tropical rainforest. New Phytol 239:576–591. https://doi.org/10.1111/nph.18973.

Kannenberg SA, Schwalm CR, Anderegg WR (2020) Ghosts of the past: how drought legacy effects shape forest functioning and carbon cycling. Ecol Lett 23:891–901. https://doi.org/10.1111/ele.13485.

Knipfer T, Reyes C, Earles JM, Berry ZC, Johnson DM, Brodersen CR, McElrone AJ (2019) Spatiotemporal coupling of vessel cavitation and discharge of stored xylem water in a tree sapling. Plant Physiol 179:1658–1668. https://doi.org/10.1104/pp.18.01303.

Knüsel S, Peters RL, Haeni M, Wilhelm M, Zweifel R (2021) Processing and extraction of seasonal tree physiological parameters from stem radius time series. Forests 12:765. https://doi.org/10.3390/f12060765.

Krejza J, Haeni M, Darenova E et al. (2022) Disentangling carbon uptake and allocation in the stems of a spruce forest. Environ Exp Bot 196:104787. https://doi.org/10.1016/j.envexpbot.2022.104787.

Lamacque L, Charrier G, dos Santos FF, Lemaire B, Améglio T, Herbette S (2020) Drought-induced mortality: branch diameter variation reveals a point of no recovery in lavender species. Plant Physiol 183:1638–1649. https://doi.org/10.1104/pp.20.00165.

Lauriks F, Salomón RL, de Roo L, Goossens W, Leroux O, Steppe K (2022) Limited plasticity of anatomical and hydraulic traits in aspen trees under elevated CO2 and seasonal drought. Plant Physiol 188: 268–284. https://doi.org/10.1093/plphys/kiab497.

Leštianska A, Fleischer P, Fleischer P, Merganičová K, Střelcová K (2020) Interspecific variation in growth and tree water status of conifers under water-limited conditions. J Hydrol Hydromech 68: 368–381. https://doi.org/10.2478/johh-2020-0028.

Liu MJ, Chen QW, Guo HN, Lyu J, Li G, Du S (2023) Daily and seasonal patterns of stem diameter micro-variations in three semi-arid forest species in relation to water status and environmental factors. Dendrochronologia 82:1266146. https://doi.org/10.1016/j.dendro.2023.126146.

Mantova M, Herbette S, Cochard H, Torres-Ruiz JM (2022) Hydraulic failure and tree mortality: from correlation to causation. Trends Plant Sci 27:335–345. https://doi.org/10.1016/j.tplants.2021.10.003.

Martinez EM, Cancela JJ, Cuesta TS, Neira XX (2011) Introduction review. Use of psychrometers in field measurements of plant material: accuracy and handling difficulties. Span J Agric Res 9: 313–328.

Martín-Gómez P, Rodríguez-Robles U, Oge J et al. (2023) Contrasting stem water uptake and storage dynamics of water-saver and water-spender species during drought and recovery. Tree Physiol 43: 1290–1306. https://doi.org/10.1093/treephys/tpad032.

Müller LM, Bahn M (2022) Drought legacies and ecosystem responses to subsequent drought. Glob Chang Biol 28:5086–5103. https://doi.org/10.1111/gcb.16270.

Novick KA, Ficklin DL, Baldocchi D et al. (2022) Confronting the water potential information gap. Nat Geosci 15:158–164. https://doi.org/10.1038/s41561-022-00909-2.

Oberhuber W, Kofler W, Schuster R, Wieser G (2015) Environmental effects on stem water deficit in co-occurring conifers exposed to soil dryness. Int J Biometeorol 59:417–426. https://doi.org/10.1007/s00484-014-0853-1.

Oberhuber W, Gruber A, Wieser G (2023) Seasonal and daily xylem radius variations in scots pine are closely linked to environmental factors affecting transpiration. Biology 12:1251. https://doi.org/10.3390/biology12091251.

Obojes N, Buscarini S, Meurer AK, Tasser E, Oberhuber W, Mayr S, Tappeiner U (2024) Tree growth at the limits: the response of multiple conifers to opposing climatic constraints along an elevational gradient in the alps. Front For Glob Change 7. https://doi.org/10.3389/ffgc.2024.1332941.

Peters RL, Steppe K, Cuny HE, De Pauw DJ, Frank DC, Schaub M, Rathgeber CB, Cabon A, Fonti P (2021) Turgor-a limiting factor for radial growth in mature conifers along an elevational gradient. New Phytol 229:213–229. https://doi.org/10.1111/nph.16872.

Peters RL, Steppe K, Pappas C et al. (2023) Daytime stomatal regulation in mature temperate trees prioritizes stem rehydration at night. New Phytol 239:533–546. https://doi.org/10.1111/nph.18964.

Pretzsch H, del Río M, Grote R, Klemmt HJ, Ordóñez C, Oviedo FB (2022) Tracing drought effects from the tree to the stand growth in temperate and Mediterranean forests: insights and consequences for forest ecology and management. Eur J For Res 141:727–751. https://doi.org/10.1007/s10342-022-01451-x.

R Core Team (2022) R: A Language and Environment for Statistical Computing. Vienna, Austria. https://www.R-project.org/.

Rehschuh R, Cecilia A, Zuber M, Faragó T, Baumbach T, Hartmann H, Jansen S, Mayr S, Ruehr N (2020) Drought-induced xylem embolism limits the recovery of leaf gas exchange in scots pine. Plant Physiol 184:852–864. https://doi.org/10.1104/pp.20.00407.

Rodriguez-Dominguez CM, Forner A, Martorell S et al. (2022) Leaf water potential measurements using the pressure chamber: synthetic testing of assumptions towards best practices for precision and accuracy. Plant Cell Environ 45:2037–2061. https://doi.org/10.1111/pce.14330.

Ruehr NK, Grote R, Mayr S, Arneth A (2019) Beyond the extreme: recovery of carbon and water relations in woody plants following heat and drought stress. Tree Physiol 39:1285–1299. https://doi.org/10.1093/treephys/tpz032.

Salomón RL, Limousin JM, Ourcival JM, Rodríguez-Calcerrada J, Steppe K (2017) Stem hydraulic capacitance decreases with drought stress: implications for modelling tree hydraulics in the Mediterranean oak *Quercus ilex*. Plant Cell Environ 40:1379–1391. https://doi.org/10.1111/pce.12928.

Salomón RL, Peters RL, Zweifel R et al. (2022) The 2018 European heatwave led to stem dehydration but not to consistent growth reductions in forests. Nat Commun 13:1–11. https://doi.org/10.1038/s41467-021-27579-9.

Sánchez-Costa E, Poyatos R, Sabaté S (2015) Contrasting growth and water use strategies in four co-occurring Mediterranean tree species revealed by concurrent measurements of sap flow and stem diameter variations. Agric For Meteorol 207:24–37. https://doi.org/10.1016/j.agrformet.2015.03.012.

Scholander PF, Bradstreet ED, Hemmingsen EA, Hammel HT (1965) Sap pressure in vascular plants. Science 148:339–346. https://doi.org/10.1126/science.148.3668.339.

Senf C, Buras A, Zang CS, Rammig A, Seidl R (2020) Excess forest mortality is consistently linked to drought across Europe. Nat Commun 11:6200. https://doi.org/10.1038/s41467-020-19924-1.

Skelton R (2020) Stem diameter fluctuations provide a new window into plant water status and function. Plant Physiol 183:1414–1415. https://doi.org/10.1104/pp.20.00897.

Skelton RP, Brodribb TJ, McAdam SA, Mitchell PJ (2017) Gas exchange recovery following natural drought is rapid unless limited by loss of leaf hydraulic conductance: evidence from an evergreen woodland. New Phytol 215:1399–1412. https://doi.org/10.1111/nph.14652.

Spinoni J, Vogt JV, Naumann G, Barbosa P, Dosio A (2018) Will drought events become more frequent and severe in Europe? Int J Climatol 38:1718–1736. http://dx.doi.org/10.1002/joc.5291.

Steppe K (2018) The potential of the tree water potential. Tree Physiol 38:937–940. https://doi.org/10.1093/treephys/tpy064.

Steppe K, De Pauw DJ, Lemeur R, Vanrolleghem PA (2006) A mathematical model linking tree sap flow dynamics to daily stem diameter fluctuations and radial stem growth. Tree Physiol 26: 257–273. https://doi.org/10.1093/treephys/26.3.257.

Steppe K, Sterck F, Deslauriers A (2015) Diel growth dynamics in tree stems: linking anatomy and ecophysiology. Trends Plant Sci 20: 335–343. https://doi.org/10.1016/j.tplants.2015.03.015.

Suarez-Gutierrez L, Müller WA, Marotzke J (2023) Extreme heat and drought typical of an end-of-century climate could occur over Europe soon and repeatedly. Commun Earth Environ 4:415. https://doi.org/10.1038/s43247-023-01075-y.

Urli M, Porté AJ, Cochard H, Guengant Y, Burlett R, Delzon S (2013) Xylem embolism threshold for catastrophic hydraulic failure in angiosperm trees. Tree Physiol 33:672–683. https://doi.org/10.1093/treephys/tpt030.

Vergeynst LL, Dierick M, Bogaerts JA, Cnudde V, Steppe K (2015) Cavitation: a blessing in disguise? New method to establish vulnerability curves and assess hydraulic capacitance of woody tissues. Tree Physiol 35:400–409. https://doi.org/10.1093/treephys/tpu056.

Yi C, Hendrey G, Niu S, McDowell N, Allen CD (2022) Tree mortality in a warming world: causes, patterns, and implications. Environ Res Lett 17:030201. https://doi.org/10.1088/1748-9326/ac507b.

Zweifel R (2015) Radial stem variations - a source of tree physiological information not fully exploited yet. Plant Cell Environ 39: 231–232. https://doi.org/10.1111/pce.12613.

Zweifel R, Item H, Häsler R (2001) Link between diurnal stem radius changes and tree water relations. Tree Physiol 21:869–877. https://doi.org/10.1093/treephys/21.12-13.869.

Zweifel R, Zimmermann L, Newbery DM (2005) Modeling tree water deficit from microclimate: an approach to quantifying drought stress. Tree Physiol 25:147–156. https://doi.org/10.1093/treephys/25.2.147.

Zweifel R, Haeni M, Buchmann N, Eugster W (2016) Are trees able to grow in periods of stem shrinkage? New Phytol 211:839–849. https://doi.org/10.1111/nph.13995.

Zweifel R, Etzold S, Basler D et al.. 2021*a*. TreeNet-the biological drought and growth indicator network. Front For Glob Change 4:776905. https://doi.org/10.3389/ffgc.2021.776905.

Zweifel R, Sterck F, Braun S, et al. 2021*b*. Why trees grow at night. New Phytol 231:2174–2185. https://doi.org/10.1111/nph.17552.

Tree Physiology, 2024, 44, tpae140
https://doi.org/10.1093/treephys/tpae140
Research paper